

# Syntheses, Structures, Luminescence, and Magnetic Properties of One-dimensional Lanthanide Coordination Polymers with a Rigid 2,2'-Bipyridine-3,3',6,6'-tetracarboxylic Acid Ligand

Baoming Ji,<sup>\*,†</sup> Dongsheng Deng,<sup>†</sup> Xiao He,<sup>†,‡</sup> Bin Liu,<sup>\*,§</sup> Shaobin Miao,<sup>†</sup> Ning Ma,<sup>†</sup> Weizhou Wang,<sup>†</sup> Liguo Ji,<sup>†,⊥</sup> Peng Liu,<sup>†,||</sup> and Xianfei Li<sup>†,¶</sup>

<sup>†</sup>College of Chemistry and Chemical Engineering, Luoyang Normal University, Luoyang 471022, People's Republic of China

<sup>‡</sup>College of Chemistry and Environmental Science, Henan Normal University, Xinxiang 453007, People's Republic of China

<sup>§</sup>Shaanxi Key Laboratory of Physico-Inorganic Chemistry, Department of Chemistry, Northwest University, Xi'an 710069, People's Republic of China

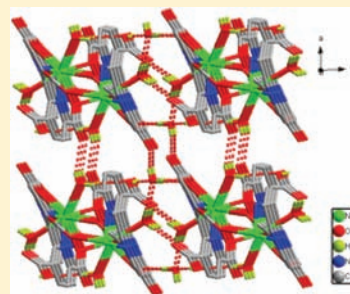
<sup>⊥</sup>College of Chemistry and Chemical Engineering, China University of Petroleum (East China), Qingdao 266555, People's Republic of China

<sup>||</sup>Department of Chemistry, Zhengzhou University, Zhengzhou 450052, People's Republic of China

<sup>¶</sup>Northwest Agriculture and Forest University, Yangling 712100, People's Republic of China

## Supporting Information

**ABSTRACT:** A series of novel one-dimensional (1-D) lanthanide coordination polymers (CPs), with the general formula  $\{[\text{Ln}(\text{bptcH})(\text{H}_2\text{O})_2]\cdot\text{H}_2\text{O}\}_n$  ( $\text{Ln} = \text{Nd}^{\text{III}}$  (1),  $\text{Eu}^{\text{III}}$  (2),  $\text{Gd}^{\text{III}}$  (3),  $\text{Tb}^{\text{III}}$  (4),  $\text{Dy}^{\text{III}}$  (5),  $\text{Ho}^{\text{III}}$  (6), or  $\text{Er}^{\text{III}}$  (7)) have been synthesized by the solvothermal reactions of the corresponding lanthanide(III) picrates and 2,2'-bipyridine-3,3',6,6'-tetracarboxylic acid (bptcH<sub>4</sub>). These polymers have been structurally characterized by single-crystal X-ray diffraction, IR, PXRD, thermogravimetric (TGA), and elemental analysis. Coordination polymers 1–7 are isostructural; they possess the same 3D supramolecular architectures and crystallize in triclinic space group  $P\bar{1}$ . The frameworks constructed from dinuclear lanthanide building blocks exhibit one-dimensional double-stranded looplike chain architectures, in which the bptcH<sup>3-</sup> ions adopted hexadentate coordination modes. The  $\text{Eu}^{\text{III}}$  (2) and  $\text{Tb}^{\text{III}}$  (4) polymers exhibit characteristic photoluminescence in the visible region. The magnetic properties of polymers 2, 3, and 5 have been investigated through the measurement of their magnetic susceptibilities over the temperature range of 1.8–300 K.



## INTRODUCTION

Crystal engineering of coordination polymers (CPs) has been the focus of research interest, not only because of the potential of these compounds as functional materials but also owing to their flexibility in aspects such as composition and topology.<sup>1</sup> Up to now, coordination polymers of various structural motifs of one-, two-, and three-dimensions (1-D, 2-D, 3-D) have been synthesized.<sup>2–4</sup> One of the focal points for the design and exploitation of such CPs is the rational choice and assembly of metal ions and versatile bridging organic ligands. As is well-known, trivalent lanthanide ions have proven particularly suitable for the construction of CPs not only due to their high coordination numbers and flexible coordination geometry but also for their unique luminescence and magnetic properties. It is commonly admitted that, for lanthanide compounds, the excellent photophysical properties are attributed to  $f-f$  transitions with an extremely narrow bandwidth.<sup>5</sup> Also, the magnetic properties of lanthanide compounds are uncommon due to the presence of strong unquenched orbital angular momentum originating from  $f$  electrons that are shielded by  $s$  and  $p$  electrons.<sup>6</sup> Many chemists synthesize lanthanide-based

CPs with many different carboxylic acids, such as aromatic acids,<sup>7</sup> aliphatic acids,<sup>8</sup> and heterocyclic acids.<sup>9</sup> Among these acids, aromatic polycarboxylic acids are the most widely used ligands due to the rigidity of the aromatic part, which favors the formation of great and ordered single crystals, and the high affinity of carboxylate function and lanthanide ion.<sup>10</sup> However, compared with di- and tricarboxylate ligands, many fewer complexes with bipyridinetetracarboxylic acids were investigated. Until now, 4,4'-bipyridine-2,2',6,6'-tetracarboxylic acid,<sup>11</sup> 2,2'-bipyridine-5,5',6,6'-tetracarboxylic acid,<sup>12</sup> and 2,2'-bipyridine-4,4',6,6'-tetracarboxylic acid have been synthesized. For these rigid ligands, various coordination modes can be adjusted to satisfy the requirements of the assembly process and interesting structural motifs may result.<sup>13–15</sup> For example, Kruger and co-workers used the 2,2'-bipyridine-4,4',6,6'-tetracarboxylic acid ligand to construct 1-D or 2-D lanthanide-based CPs.<sup>13,14</sup> Investigation has revealed that the structures of lanthanide CPs based on 2,2'-bipyridine-4,4',6,6'-tetracarboxylic

Received: September 23, 2011

Published: February 2, 2012

Table 1. Crystallographic Data and Structure Refinement Summary for Complexes 1–7

	1	2	3	4	5	6	7
formula	C <sub>14</sub> H <sub>11</sub> NdN <sub>2</sub> O <sub>11</sub>	C <sub>14</sub> H <sub>11</sub> EuN <sub>2</sub> O <sub>11</sub>	C <sub>14</sub> H <sub>11</sub> N <sub>2</sub> GdO <sub>11</sub>	C <sub>14</sub> H <sub>11</sub> N <sub>2</sub> TbO <sub>11</sub>	C <sub>14</sub> H <sub>11</sub> N <sub>2</sub> DyO <sub>11</sub>	C <sub>14</sub> H <sub>11</sub> HoN <sub>2</sub> O <sub>11</sub>	C <sub>14</sub> H <sub>11</sub> ErN <sub>2</sub> O <sub>11</sub>
<i>M</i>	527.49	535.21	540.50	542.17	545.75	548.18	550.51
cryst syst	triclinic	triclinic	triclinic	triclinic	triclinic	triclinic	triclinic
space group	<i>P</i> $\bar{1}$	<i>P</i> $\bar{1}$	<i>P</i> $\bar{1}$	<i>P</i> $\bar{1}$	<i>P</i> $\bar{1}$	<i>P</i> $\bar{1}$	<i>P</i> $\bar{1}$
<i>a</i> (Å)	9.2072(12)	9.2247(11)	9.2249(11)	9.236(6)	9.2185(11)	9.1986(11)	9.1813(11)
<i>b</i> (Å)	9.3200(12)	9.2792(11)	9.2640(11)	9.236(6)	9.2289(11)	9.2305(11)	9.2376(11)
<i>c</i> (Å)	9.4981(12)	9.4629(11)	9.4434(11)	9.447(6)	9.4132(11)	9.3993(12)	9.3885(11)
$\alpha$ (deg)	86.1740(10)	86.1680(10)	86.2070(10)	87.255(6)	87.1670(10)	86.9970(10)	86.8560(10)
$\beta$ (deg)	88.2810(10)	87.7610(10)	87.6560(10)	86.232(6)	86.2270(10)	86.2330(10)	86.2240(10)
$\gamma$ (deg)	84.7320(10)	85.2170(10)	85.3200(10)	85.446(6)	85.6640(10)	85.7400(10)	85.8460(10)
<i>V</i> (Å <sup>3</sup> )	809.56(18)	804.92(16)	802.06(16)	800.8(8)	796.02(16)	793.24(17)	791.45(16)
<i>Z</i>	2	2	2	2	2	2	2
<i>D</i> <sub>calc</sub> (g cm <sup>-3</sup> )	2.164	2.208	2.238	2.248	2.277	2.295	2.310
$\mu$ (mm <sup>-1</sup> )	3.277	3.967	4.205	4.486	4.765	5.059	5.374
<i>F</i> (000)	514	520	522	524	526	528	530
data/params	6232/3001	6174/2978	6149/2972	6149/2968	6085/2944	5926/2931	5910/2925
GOF on <i>F</i> <sup>2</sup>	1.048	1.054	1.022	1.037	1.062	1.042	1.020
<i>R</i> <sub>1</sub> ( <i>I</i> > 2 $\sigma$ )	0.0223	0.0258	0.0166	0.0167	0.0182	0.0181	0.0177
<i>wR</i> <sub>2</sub> ( <i>I</i> > 2 $\sigma$ )	0.0495	0.0631	0.0424	0.0428	0.0456	0.0443	0.0448

acid ligand are very similar when consideration is given to the La(III) coordination number and geometry, and each link together to form topologically identical 1-D polymeric chains through 4- and 4'-carboxylate group bridging. More recently, Pruchnik and co-workers reported two transition-metal complexes (Fe<sup>2+</sup> and Co<sup>2+</sup>) of 2,2'-bipyridine-3,3',6,6'-tetracarboxylic acid,<sup>16</sup> but its lanthanide complexes have been unexplored up to now. However, the presence of four potential coordinating carboxylate groups in the bipyridinetetracarboxylate anion together with the variety of coordination numbers of the metal ions accounts for the difficulties in the structural predictions of the corresponding complexes. Therefore, further research is necessary to enrich and develop this field.

In this work, the selection of 2,2'-bipyridine-3,3',6,6'-tetracarboxylic acid ligand (bptcH<sub>4</sub>) was based on the following considerations: (1) under appropriate conditions, bptcH<sub>4</sub> can completely or partially deprotonate and adopt various coordination modes when it coordinates to metals and thus may produce various structural topologies; (2) due to the instinctive high oxophilicity of the lanthanide ions, the bptcH<sub>4</sub> is an ideal ligand in constructing lanthanide CPs; (3) the pyridine ring and two carboxylic groups on 6- and 6'-positions can chelate the lanthanide ions safely to afford stable structures, while the other two carboxylic groups on 3- and 3'-positions can bridge the other metal center to form chain-like units with Ln–O–Ln connectivity; (4) the carboxylate groups can act not only as a hydrogen bond acceptors but also as hydrogen bond donors, depending on the degree of deprotonation; and (5) bptcH<sub>4</sub> is a polydentate ligand with a scissor-shaped backbone, and this allows a certain degree of rotation to modulate the intermetallic distances so as to develop potential magnetic materials. Herein, we use 2,2'-bipyridine-3,3',6,6'-tetracarboxylic acid (bptcH<sub>4</sub>) as a multidentate bridging ligand to construct novel lanthanide CPs under hydrothermal conditions. The syntheses, crystal structures, and properties of seven 1-D lanthanide CPs {[Ln(bptcH)(H<sub>2</sub>O)<sub>2</sub>]}<sub>n</sub> (Ln = Nd (1), Eu (2), Gd (3), Tb (4), Dy (5), Ho (6), or Er (7)) will be presented.

## EXPERIMENTAL SECTION

**Materials and Physical Techniques.** 2,2'-Bipyridine-3,3',6,6'-tetracarboxylic acid (bptcH<sub>4</sub>) was synthesized according to the literature method.<sup>16</sup> Hydrated lanthanide picrates were prepared by the reactions of the corresponding lanthanide oxides and picric acid. The result of elemental analysis indicated that the stoichiometric formula of lanthanide picrates is Ln(Pic)<sub>3</sub>·11H<sub>2</sub>O. All other chemicals were commercially purchased and used without further purification. The IR spectra were recorded as KBr pellets on a Nicolet Avatar-360 spectrometer in the 4000–400 cm<sup>-1</sup> region. Elemental analyses for C, H, and N were carried out on a Flash 2000 elemental analyzer. Powder X-ray diffraction (PXRD) measurements were performed on a Bruker D8-ADVANCE X-ray diffractometer with Cu K $\alpha$  radiation ( $\lambda$  = 1.5418 Å). Thermogravimetric analyses were carried out on a SDT Q600 thermogravimetric analyzer. A platinum pan was used for heating the sample with a heating rate of 10 °C/min under a N<sub>2</sub> atmosphere. Luminescent spectra were recorded with a Hitachi F4500 fluorescence spectrophotometer. The magnetic measurements in the temperature range of 1.8–300 K were carried out on a Quantum Design MPMS7 SQUID magnetometer. Diamagnetic corrections were made with Pascal's constants for all samples.

**Synthesis of the Complexes.** All seven complexes were prepared by the same method, as follows: a mixture of Ln(Pic)<sub>3</sub>·11H<sub>2</sub>O (Ln = Nd, Eu, Gd, Tb, Dy, Ho, and Er, 0.2 mmol), bptcH<sub>4</sub> ligand (0.2 mmol), and H<sub>2</sub>O (10 mL) was sealed in a 23 mL Teflon-lined stainless steel container and heated at 150 °C for 3 days, then cooled to room temperature at a rate of 5 °C h<sup>-1</sup>. Crystals of 1–7 suitable for a single-crystal X-ray diffraction study were isolated by filtration and washed with DMF several times. For 1, yield: 0.080 g, 76% based on Nd. Anal. Calcd (%) for C<sub>14</sub>H<sub>11</sub>NdN<sub>2</sub>O<sub>11</sub>: C, 31.88; H, 2.10; N, 5.31. Found: C, 32.07; H, 2.31; N, 5.16. IR (KBr, cm<sup>-1</sup>): 3494(m), 3438(m), 2918(w), 1715(w), 1644(s), 1596(s), 1461(m), 1402(s), 1362(s), 1308(m), 1232(m), 1181(m), 1083(m), 796(m). For 2, yield: 0.071 g, 66% based on Eu. Anal. Calcd (%) for C<sub>14</sub>H<sub>11</sub>EuN<sub>2</sub>O<sub>11</sub>: C, 31.42; H, 2.07; N, 5.23. Found: C, 31.53; H, 2.19; N, 5.07. IR (KBr, cm<sup>-1</sup>): 3499(m), 3422(m), 3081(m), 2920(w), 1716(m), 1650(s), 1597(s), 1462(m), 1404(m), 1363(m), 1306(m), 1233(m), 1181(m), 1084(m), 773(m). For 3, yield: 0.079 g, 73% based on Gd. Anal. Calcd (%) for C<sub>14</sub>H<sub>11</sub>GdN<sub>2</sub>O<sub>11</sub>: C, 31.11; H, 2.05; N, 5.18. Found: C, 31.34; H, 2.13; N, 5.01. IR (KBr, cm<sup>-1</sup>): 3501(m), 3427(m), 3082(m), 2919(w), 1714(m), 1653(s), 1593(s), 1459(m), 1401(m), 1367(m), 1302(m), 1219(m), 1180(m), 1087(m), 779(m). For 4, yield: 0.073 g, 67% based on Tb. Anal. Calcd (%) for C<sub>14</sub>H<sub>11</sub>TbN<sub>2</sub>O<sub>11</sub>: C, 31.01; H, 2.04; N, 5.17. Found: C, 30.89; H, 2.10; N, 4.99. IR (KBr, cm<sup>-1</sup>): 3503(m),

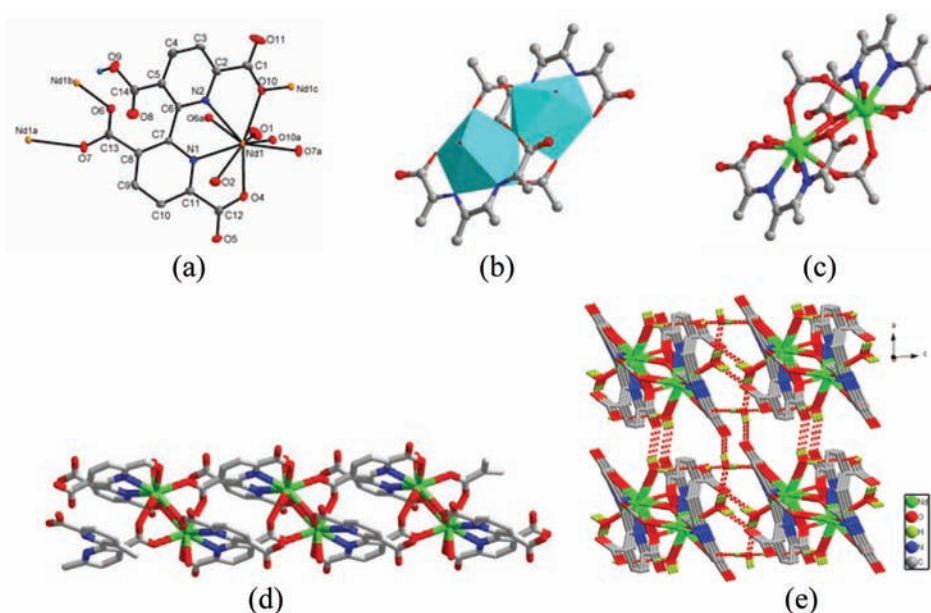


**Figure 1.** (a) The coordination environments and atomic numbering scheme for **1** with symmetry equivalents of Nd1 given to show further coordination of the carboxylate oxygen atoms. Bipyridyl and water molecule hydrogen atoms omitted for clarity. Symmetry operators:  $a = x, y + 1, z$ ;  $b = -x + 1, -y + 1, -z + 1$ ;  $c = -x + 1, -y + 2, -z + 1$ . (b) Polyhedral representation and (c) ball and stick of dinuclear building block in **1**. (d) View of a one-dimensional double-stranded looplike chain structure in **1**. Bipyridyl hydrogen atoms, water molecule hydrogen atoms, and lattice water molecule omitted for clarity. (e) Three-dimensional network in **1**. The extensive hydrogen bonds are colored red.

3418(m), 3079(m), 2924(w), 1708(m), 1649(s), 1592(s), 1464(m), 1398(m), 1362(m), 1300(m), 1215(m), 1176(m), 1081(m), 774(m). For **5**, yield: 0.076 g, 69% based on Dy. Anal. Calcd (%) for  $C_{14}H_{11}DyN_2O_{11}$ : C, 30.81; H, 2.03; N, 5.13. Found: C, 31.07; H, 2.15; N, 5.01. IR (KBr,  $cm^{-1}$ ): 3491(m), 3415(m), 3226(m), 2919(w), 1714(m), 1650(s), 1598(s), 1464(s), 1408(m), 1364(s), 1308(m), 1234(m), 1182(m), 1086(m), 772(m). For **6**, yield: 0.083 g, 75% based on Ho. Anal. Calcd (%) for  $C_{14}H_{11}HoN_2O_{11}$ : C, 30.67; H, 2.02; N, 5.11. Found: C, 30.49; H, 2.16; N, 5.23. IR (KBr,  $cm^{-1}$ ): 3416(m), 3415(m), 3088(w), 2926(w), 1715(m), 1650(s), 1598(s), 1463(m), 1409(s), 1364(s), 1308(m), 1234(m), 1182(m), 1086(m), 773(m). For **7**, yield: 0.077 g, 70% based on Er. Anal. Calcd (%) for  $C_{14}H_{11}ErN_2O_{11}$ : C, 30.54; H, 2.01; N, 5.09. Found: C, 30.31; H, 2.19; N, 4.93. IR (KBr,  $cm^{-1}$ ): 3488(m), 3432(m), 2925(w), 1713(w), 1650(s), 1600(s), 1463(m), 1408(s), 1365(s), 1308(m), 1235(m), 1182(m), 1086(m), 774(m).

**X-ray Structural Studies.** Crystallographic data for **1–7** were collected on a Bruker Smart Apex-II CCD area detector equipped with a graphite-monochromatic Mo  $K\alpha$  radiation ( $\lambda = 0.71073 \text{ \AA}$ ) at room temperature. An empirical absorption correction was applied. All structures were solved and refined by a combination of direct methods and difference Fourier syntheses, using SHELXTL.<sup>17,18</sup> Anisotropic thermal parameters were assigned to all non-hydrogen atoms. The hydrogen atoms were set in calculated positions and refined as riding atoms with a common isotropic thermal parameter. The crystallographic data for **1–7** are listed in Table 1; CCDC 809308 (**1**), 809309 (**2**), 809310 (**3**), 809311 (**4**), 809312 (**5**), 809313 (**6**), and 809314 (**7**) contain the supplementary crystallographic data. These data can be obtained free of charge via [www.ccdc.cam.ac.uk/conts/retrieving.html](http://www.ccdc.cam.ac.uk/conts/retrieving.html) (or from the Cambridge Crystallographic Data Center, 12 Union Road, Cambridge CB2 1EZ, UK. Fax: (44) 1223 336-033. E-mail: [deposit@ccdc.cam.ac.uk](mailto:deposit@ccdc.cam.ac.uk)).

## RESULTS AND DISCUSSION

**Synthesis.** The coordination polymers of **1–7** were successfully synthesized by the reaction of  $bptcH_4$  and the corresponding lanthanide picrates under hydrothermal conditions. However, suitable crystals were not obtained when we tried to synthesize these complexes by the use of traditional methods

such as slow evaporation and diffusion at room temperature. This may be attributed to the competitive advantage of hydrothermal synthesis, a special environment with high temperature and pressure, which induced the generation of large crystals. The structural evidence demonstrates that the multidentate  $bptcH_4$  ligand is capable of binding trivalent lanthanide atoms into polymeric  $Ln^{3+}$  prisms. The carboxylate ligand, as a hard Lewis base, is able to form strong bonds with lanthanide ions. Additionally, as a polydentate chelator, such ligands are sufficient to satisfy the high (8, 9, or more) coordination numbers usually required by  $Ln^{3+}$  ions.

**Crystal Structures of 1–7.** The X-ray structure analyses reveal that polymers **1–7** are isostructural, so only the structure of **1** is described in detail. Framework **1** is a 1-D chainlike coordination polymer consisting of dinuclear lanthanide building blocks, similar to the previous reports.<sup>7a</sup> The atomic numbering scheme and atom connectivity for **1** are shown in Figure 1a. Polymer **1** crystallizes in triclinic  $P\bar{1}$  space group, and crystallographic data are shown in Table 1. The asymmetric unit contains one crystallographically independent Nd(III) atom, one  $bptcH^{3-}$  ion, two coordination water molecules, and one lattice water molecule. The Nd(III) center coordinated to five O atoms [O(4), O(6)i, O(7)ii, O(10), and O(10)iii] belonging to four symmetry-related  $bptcH^{3-}$  ions and two bipyridyl nitrogen atoms [N(1) and N(2)] belonging to one  $bptcH^{3-}$  ion, plus two O atoms of two water molecules [O(1) and O2]. As is well-known, the pH value plays a crucial role in the structure formation.<sup>19</sup> Under the experimental conditions, for each  $bptcH_4$  ligand, there is one carboxyl group that is not deprotonated. As a result, each Nd atom is linked with four  $bptcH^{3-}$  ligands, and in turn, each  $bptcH^{3-}$  ligand is linked with four Nd atoms. O(10) coordinates one Nd(III) ion and also participates in unidentate bridging of another Nd(III) ion. This leads to a nine-coordination sphere,  $\{NdN_2O_7\}$  [Figure 1a; symmetry operations: ((i) =  $-x + 1, -y + 1, -z + 1$ ); (ii) =  $x, y + 1, z$ ); (iii) =  $-x + 1, -y + 2, -z + 1$ )], which resembles a



highly distorted tricapped trigonal geometry (Figure 2b). The Nd–O bond lengths are in the range from 2.426(2) to 2.575(2) Å, and

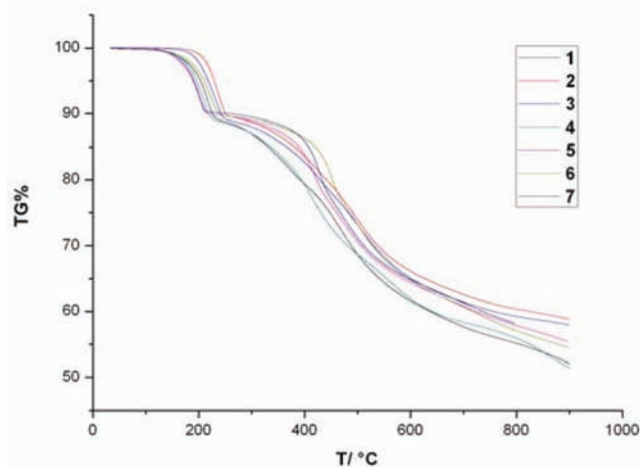


Figure 2. Thermogravimetric analyses (TGA) curve of polymers 1–7.

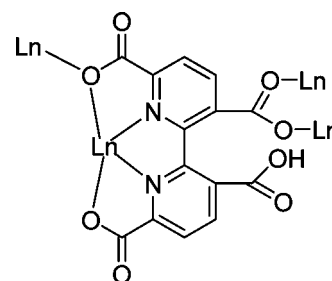
the Nd–N bond distances are 2.616(3) and 2.634(3) Å, which are similar to the reported Nd–O and Nd–N bond distances.<sup>7a,10</sup> The average distance of Nd–O is 2.355 Å, which is strikingly shorter than that of Nd–N (2.554 Å) (Supporting Information, Table S1). Additionally, the distortion of the lanthanide coordination sphere is clearly reflected by the internal (N,O)–Nd–(N,O) bond angles: while the O–Nd–O angles range between 66.80(8)° and 152.36(2)°, the O–Nd–N angles can be found in the 64.09°–150.06(8)° range, and the N–Nd–N angle is 60.01(8)° (Supporting Information, Table S1). The dihedral angle between two pyridyl rings is 28.63°, whereas the three 6, 6', and 3 carboxylate groups (centered about C1, C12, and C13), which participated in coordination with Nd are twisted by 3.97°, 10.14°, and 23.59°, respectively, with respect to the pyridyl rings to which they are attached. The 3' carboxylate group (centered C13), which remained uncoordinated and in a protonated state, is twisted by 36.32(3)°.

In the crystal structure, two crystallographically equivalent Nd atoms are bridged by four carboxylate groups form four  $\text{bptcH}^{3-}$  ions in didmonodentate and monodidentate fashions to give a dinuclear lanthanide building block  $[\text{Nd}_2\text{N}_4(\text{CO}_2\text{R})_6]$  with shorter separations of Nd...Nd (3.999 Å). The dinuclear lanthanide building blocks are connected to each other through  $\text{bptcH}^{3-}$  leading to a 1-D double-stranded looplike chain (Figure 1d). Considering that there are two coordinated water molecules and a lattice water molecule within the structure, the packing of compound 1 in the crystal lattice is worth mentioning. Each 1-D double-stranded looplike chain interacts with neighboring ones via O–H...O hydrogen bonds, forming extended 3-D structures. First, O–H...O hydrogen bonds formed between coordinated water molecules (O2) of one chain and carboxylate oxygen atoms of an adjacent chain (O11) (O...O, 2.810(4) Å), which link each chain to two adjacent chains into a 2-D hydrogen-bonded network. Finally, uncoordinated water molecules (O3) hydrogen bond to three carboxylate oxygen atoms (O4, O5, O9; O...O 2.800(3), 2.695(3), 2.592(3) Å, respectively) and coordinated water molecules (O1; O...O, 2.871(4) Å) of adjacent sheets, and coordinated water molecules (O1) hydrogen bond to carboxylate oxygen atoms (O8; O...O, 2.807(4) Å), thereby linking adjacent sheets to form a complicated 3-D hydrogen-bonded network, as

shown in Figure 1e. Details of the hydrogen bond interactions are reported in Table S2, Supporting Information.

**Structural Features of the Polymers 1–7.** For the seven novel lanthanide CPs reported in this study, the same structural feature is that the frameworks are constructed by one kind of dinuclear lanthanide building blocks (Supporting Information, Figure S1–S7), and they possess the same 3D architectures and crystallize in triclinic space group  $P\bar{1}$ . Because the structures of the dinuclear building blocks in 1–7 are very similar to each other, the polymers 1–7 display very similar crystal cell parameters (Table 1). In 1–7, the  $\text{bptcH}_4$  ligands adopt the same coordinated modes (Scheme 1), and this should be the main

Scheme 1. The Coordination Modes of  $\text{bptcH}^{3-}$



role in the formation of 1-D double-stranded looplike chain. Moreover, the coordinated or crystalline water molecules and carboxylate oxygen atoms are the main part of hydrogen-bonded motifs. The lattice water molecules of all seven complexes contribute to bridge the adjacent sheet to a 3-D network with hydrogen bonds. Thus, the strong O–H...O hydrogen bonds play an important role in contributing to the stability of the 3-D framework solids. It is noted that the lanthanide contraction effect is observed in the seven lanthanide CPs. We have compared the average Ln–N and Ln–O bond lengths among the complexes 1–7 (Supporting Information, Table S1). The average lengths between the lanthanide and N atoms decrease continuously from 2.625(3) to 2.528(2) Å, and the average lengths between the lanthanide and O atoms also decrease continuously from 2.491(2) to 2.406(2) Å. This result is similar to previous reports.<sup>10a,b</sup> Furthermore, in the dinuclear lanthanide building blocks, the Ln–Ln distances also decrease continuously from 3.999 Å in 1 to 3.949 Å in 2, 3.933 Å in 3, 3.918 Å in 4, 3.900 Å in 5, 3.886 Å in 6, and 3.874 Å in 7.

**Thermal Stability and Powder X-ray Diffraction.** The thermal stability of polymers 1–7 was examined by thermogravimetric analyses (TGA) in the 30–900 °C range. Thermograms show similar profiles and are provided as Figure 2. The compounds are thermally stable up to 150 °C, with the first weight loss between 152 and 210 °C (10.58% for 1, 10.45% for 2, 10.32% for 3, 10.26% for 4, 10.05% for 5, 10.03% for 6, and 10.02% for 7), corresponding to the release of one lattice water molecule and two coordinated water molecules (calcd 10.23% for 1, 10.08 for 2, 9.99 for 3, 9.96 for 4, 9.87% for 5, 9.85% for 6, and 9.84% for 7). The second weight loss, between 290 and 610 °C (62.28% for 1, 61.79% for 2, 61.39% for 3, 61.22% for 4, 60.26% for 5, 60.32% for 6, and 60.15% for 7), is attributed to the thermal decomposition of the organic components (calcd 62.37% for 1, 61.38% for 2, 60.87% for 3, 60.68% for 4, 60.14% for 5, 60.04% for 6, and 59.93% for 7), leading to the formation of the corresponding  $\text{Ln}_2\text{O}_3$ .

PXRD patterns were measured on bulk crystalline powders from the large-scale syntheses of the lanthanide complexes suspended in their mother liquor. The experimental PXRD patterns of complexes 1–7 are in agreement with that simulated from the single-crystal data, as shown in Figure 3. This result shows the phase purity of the bulk samples.

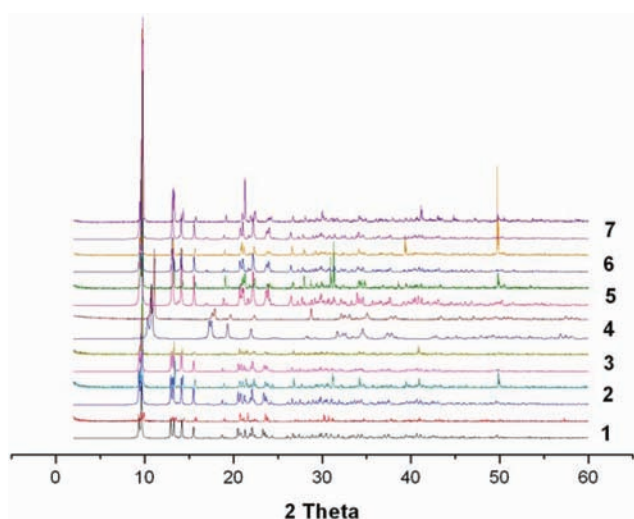


**Figure 3.** Comparison of the experimental and simulated PXRD patterns. In each group, the top is the experimental pattern, and the bottom is the simulated one.

**IR Spectrum.** The IR spectra of complexes 1–7 have been measured. It is noted that the IR spectra of 1–7 are fully identical, suggesting that the seven complexes may be

isostructural and the  $\text{bptcH}^{3-}$  ions are in the same coordination modes, which was further confirmed by the X-ray diffraction analysis. The characteristic bands of the carboxylic acid groups in 1–7 are shown in ca.  $1714\text{ cm}^{-1}$  for asymmetric stretching and ca.  $1363\text{ cm}^{-1}$  for symmetric stretching. The features at ca.  $1650$  and  $1597\text{ cm}^{-1}$  are attributed to the asymmetric stretching vibrations for carboxylate groups ( $\nu_{\text{as}}(\text{COO}^-)$ ), and the characteristic bands observed at ca.  $1463$  and  $1408\text{ cm}^{-1}$  can be regarded as the symmetric stretching vibrations of carboxylate groups ( $\nu_{\text{s}}(\text{COO}^-)$ ),<sup>20</sup> which suggests that the carboxylate groups are in differing coordination environments. Indeed, the peak separation between  $\nu_{\text{as}}(\text{COO}^-)$  and  $\nu_{\text{s}}(\text{COO}^-)$  of the carboxylate groups has a value of  $\Delta = 187\text{ cm}^{-1}$  and may be due to the presence of a bridging carboxylate group.<sup>14</sup> In addition, for 1–7, a narrow band is visible above  $3400\text{ cm}^{-1}$  (maximum peaking at  $3499\text{ cm}^{-1}$ ) associated with the highly defined environment of the H-bonded water molecules as depicted by the crystal structures.

**Photoluminescence Studies.** Taking into account the excellent luminescent properties of  $\text{Eu}^{3+}$  and  $\text{Tb}^{3+}$  ions, the luminescence of their polymers and  $\text{bptcH}_4$  were investigated. As shown in Figure 4a, the free  $\text{bptcH}_4$  ligand shows an emission band at  $508\text{ nm}$  ( $\lambda_{\text{ex}} = 400\text{ nm}$ ) and  $535\text{ nm}$  ( $\lambda_{\text{ex}} = 340\text{ nm}$ ), which is attributed to the  $\pi \rightarrow \pi^*$  transitions. Upon excitation at  $400\text{ nm}$ , compound 2 exhibits typical emission bands of  $\text{Eu}^{3+}$  ions, whereas the emission band from the free ligand is not observed, indicating energy transfer from the ligand to the  $\text{Eu}^{3+}$  center during photoluminescence. The emission bands in compound 2 arise from of  ${}^5\text{D}_0 \rightarrow {}^7\text{F}_j$  ( $J = 0-4$ ) of  $\text{Eu}^{3+}$  at the peaks of  $580, 594, 616, 650,$  and  $697\text{ nm}$ , respectively, as shown in Figure 4b. The symmetry-forbidden transition of  ${}^5\text{D}_0 \rightarrow {}^7\text{F}_0$  ( $580\text{ nm}$ ) indicates that the  $\text{Eu}^{3+}$  ions in 2 possess a noncentrosymmetric coordination environment.<sup>21</sup> The intensity of

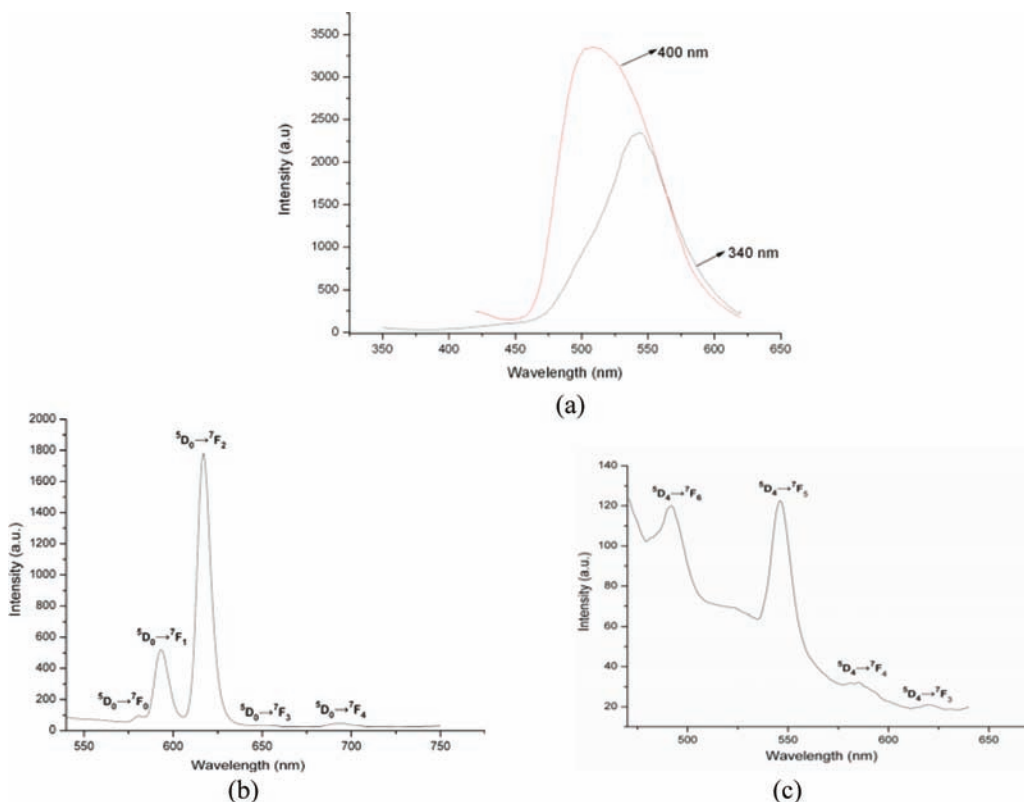


**Figure 4.** Emission spectra of the ligand  $\text{bptcH}_4$  (a) and complexes 2 (a) and 4 (c).

the  $^5D_0 \rightarrow ^7F_2$  transition (electric dipole) is ca. 3.5 times the intensity of the  $^5D_0 \rightarrow ^7F_1$  transition (magnetic dipole), which suggests low symmetry of the Eu center<sup>5a,22</sup> and is consistent with the results from crystallographic analyses. In addition, the red emission of  $^5D_0 \rightarrow ^7F_2$  transition is the most intense, which suggests that the ligands are suitable for the sensitization of red luminescence for  $\text{Eu}^{3+}$  ion under the experimental conditions, as observed in the previous report.<sup>21b</sup> Upon excitation at 340 nm, the emission spectrum of **4** (Figure 4c) exhibits the four characteristic emissions of  $\text{Tb}^{3+}$ . They are assigned to the  $^5D_4 \rightarrow ^7F_j$  ( $J = 3, 4, 5, 6$ ),  $^5D_4 \rightarrow ^7F_6$  (491 nm),  $^5D_4 \rightarrow ^7F_5$  (546 nm),  $^5D_4 \rightarrow ^7F_4$  (584 nm), and  $^5D_4 \rightarrow ^7F_j$  (620 nm) transitions. However, there is a very intense broad background in the excitation spectrum of **4**, which means there exists intramolecular  $\pi \rightarrow \pi^*$  transition of ligands.

**Magnetic Properties.** Variable-temperature magnetic susceptibility measurements were performed on powder samples of **2**, **3**, and **5** in the temperature range of 1.8–300 K. Figure 5

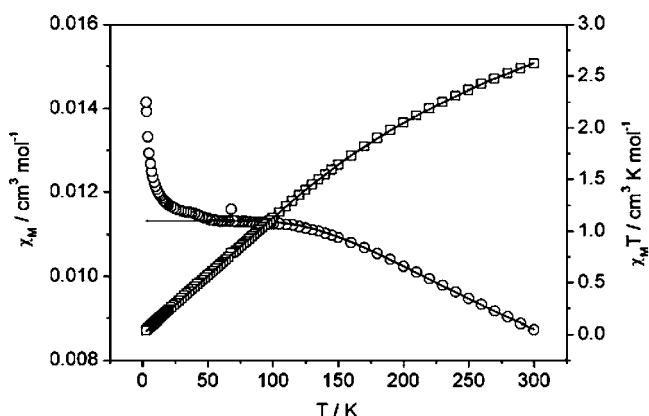


Figure 5. Plots of  $\chi_M T$  and  $\chi_M$  vs  $T$  for **2**.

shows  $\chi_M T$  and  $\chi_M$  vs  $T$  plots for compound **2**. The  $\chi_M T$  value at room temperature is  $2.62 \text{ cm}^3 \text{ K mol}^{-1}$  per  $\text{Eu}(\text{III})_2$ , close to what is previously reported in the free-ion approximation,<sup>23</sup> and  $\chi_M T$  decreases gradually upon cooling the sample and reaches  $0.039 \text{ cm}^3 \text{ K mol}^{-1}$  at 1.8 K. The shape of these curves is a typical characteristic occurrence of thermally populated excited states. For  $\text{Eu}^{3+}$ , the  $^7F$  ground term is split by the spin-orbit coupling ( $\hat{H} = \lambda L \cdot S$ ) into seven states  $^7F_j$  ( $J = 0, 1, \dots, 6$ ). The  $^7F_0$  ground state is taken as the origin, and  $\lambda$  is small enough for the first excited states to be thermally populated; in addition, the  $g_j$  factors are equal to 1.5, except  $g_0$  which is equal to  $S$ , and the magnetic susceptibility can be expressed as

$$\chi_{\text{Eu}} = \frac{N\beta^2}{3kx(T - \theta)} [24 + (27x/2 - 3/2)e^{-x} + (135x/2 - 5/2)e^{-3x} + (189x - 7/2)e^{-6x} + (405x - 9/2)e^{-10x} + (1485x/2 - 11/2)e^{-15x} + (2457x/2 - 13/2)e^{-21x}] / [1 + 3e^{-x} + 5e^{-3x} + 7e^{-6x} + 9e^{-10x} + 11e^{-15x} + 13e^{-21x}]$$

with  $x = \lambda/(kT)$ , where  $N$  is Avogadro's number,  $\beta$  is the Bohr magneton,  $k$  is the Boltzmann constant, and the Weiss constant  $\theta$  accounts for the magnetic interactions between neighboring  $\text{Eu}^{3+}$  ions. The best fit, shown as the solid line in Figure 5, gives parameters  $\lambda = 349 \text{ cm}^{-1}$ ,  $\theta = -1.14 \text{ K}$ . The negative  $\theta$  value

confirms the presence of weak antiferromagnetic interactions between  $\text{Eu}^{3+}$  ions.

The measurements performed on compound **3** are shown in Figure 6. The SQUID measurement shows a  $\chi_M T$  value at room

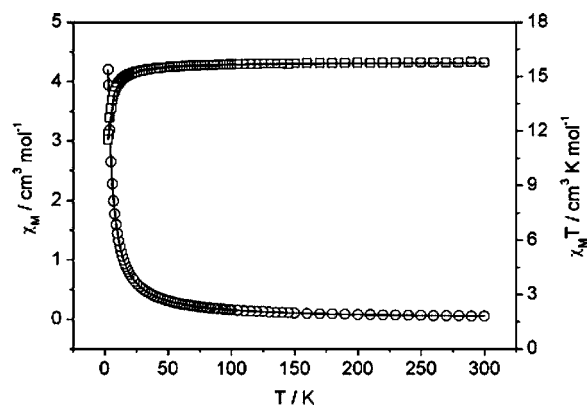


Figure 6. Plots of  $\chi_M T$  and  $\chi_M$  vs  $T$  for **3**.

temperature of  $15.76 \text{ cm}^3 \text{ K mol}^{-1}$ , corresponding to the value expected for two  $\text{Gd}(\text{III})$  ion, which has a  $S = 7/2$  ground state. The value remains roughly constant until about 50 K, where an abrupt decrease is clearly visible, reaching a value of  $11.52 \text{ cm}^3 \text{ K mol}^{-1}$  at 1.8 K. The spin-exchange integral of the compound **3** was analyzed using a spin-only expression described by the spin Hamiltonian  $\hat{H} = -2J\text{S}_1 \cdot \text{S}_2$ . The experimental data were fit using the following equation:

$$\chi = \frac{2Ng^2\beta^2}{k(T - \theta)} \times [140e^{56J/(kT)} + 91e^{42J/(kT)} + 55e^{30J/(kT)} + 30e^{20J/(kT)} + 14e^{12J/(kT)} + 5e^{6J/(kT)} + e^{2J/(kT)}] / [15e^{56J/(kT)} + 13e^{42J/(kT)} + 11e^{30J/(kT)} + 9e^{20J/(kT)} + 7e^{12J/(kT)} + 5e^{6J/(kT)} + 3e^{2J/(kT)} + 1]$$

$\theta$  is a correction term for the magnetic interactions between neighboring  $\text{Gd}^{3+}$  ions. The best fit gives parameters  $g = 2.003$ ,  $J = -0.04 \text{ cm}^{-1}$ , and  $\theta = -0.008 \text{ K}$ . The negative  $\theta$  value confirms the presence of weak antiferromagnetic interactions between  $\text{Gd}^{3+}$  ions.

In Figure 7, the plot of  $\chi_M T$  vs  $T$  for a powder sample of **5** is presented. At room temperature, the  $\chi_M T$  value is equal to

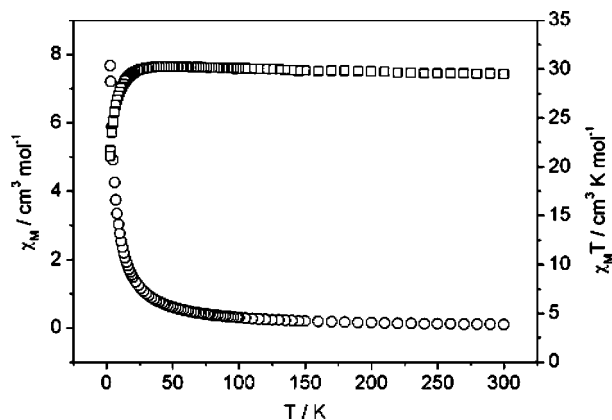


Figure 7. Plots of  $\chi_M T$  and  $\chi_M$  vs  $T$  for **5**.



29.46 cm<sup>3</sup> K mol<sup>-1</sup>, which corresponds to the value calculated for two isolated Dy<sup>3+</sup> ( $J = 15/2$ ,  $g_J = 4/3$ ). As the temperature is lowered, the  $\chi_{MT}$  gradually increases to reach a dispersed maximum of 30.25 cm<sup>3</sup> K mol<sup>-1</sup> at  $T \approx 52$  K and then abruptly decreases to the value of 21.07 cm<sup>3</sup> K mol<sup>-1</sup> at 1.8 K. The maximum  $\chi_{MT}$  value may be related to a ferromagnetic exchange between the magnetic centers.

## CONCLUSIONS

In summary, we have successfully assembled the lanthanide(III) ions and bptcH<sub>4</sub> into seven lanthanide coordination polymers: {[Ln-(bptcH)(H<sub>2</sub>O)<sub>2</sub>·H<sub>2</sub>O]}<sub>n</sub> (Ln = Nd (1), Eu (2), Gd (3), Tb (4), Dy (5), Ho (6), or Er (7)). Single-crystal X-ray diffraction analysis revealed that the same coordination modes of the organic bridge ligand and the same coordination numbers of lanthanide atoms could promote the same topology structures, which are constructed from similar dinuclear lanthanide building blocks. The coordination polymers 1–7 possess 1-D double-stranded looplike chain structures that are further interlinked into a 3-D supramolecular network based on hydrogenbonding interactions. Compound 2 exhibits strong red emission, and 4 has pure green luminescence and thus can be a good candidate for green-light emitting diode devices.<sup>24</sup> Furthermore, polymers 2, 3, and 5 display antiferromagnetic interactions, suggesting that these compounds may be efficient solid emitting and antiferromagnetic materials.

## ASSOCIATED CONTENT

### Supporting Information

Selected bond distances and angles, geometrical parameters of hydrogen bonds, dinuclear lanthanide building blocks, and crystallographic information files for polymers 1–7. This material is available free of charge via the Internet at <http://pubs.acs.org>.

## AUTHOR INFORMATION

### Corresponding Author

\*E-mail addresses: [lyhxxjbm@126.com](mailto:lyhxxjbm@126.com); [liubin@nwu.edu.cn](mailto:liubin@nwu.edu.cn).

## ACKNOWLEDGMENTS

We are grateful to the Natural Science Foundation of China (Grant Nos. 20872057 and 21072089) and the Natural Science Foundation of Henan Province (Grant No. 082300420040) for the financial support.

## REFERENCES

- (1) (a) Batten, S. R.; Neville, S. M.; Turner, D. R. *Coordination Polymers: Design, Analysis and Application*; Royal Society of Chemistry: Cambridge, U.K., 2009. (b) Férey, G. *Chem. Soc. Rev.* **2008**, *37*, 191. (c) Férey, G.; Mellot-Draznieks, C.; Serre, C.; Millange, F. *Acc. Chem. Res.* **2005**, *38*, 217. (d) James, S. L. *Chem. Soc. Rev.* **2003**, *32*, 276. (e) Moulton, B.; Zaworotko, M. J. *Chem. Rev.* **2001**, *101*, 1629.
- (2) (a) Harbuzaru, B. V.; Corma, A.; Rey, F.; Atienzar, P.; Jorda, J. L.; Garcia, H.; Ananias, D.; Carlos, L. D.; Rocha, J. *Angew. Chem., Int. Ed.* **2008**, *47*, 1080. (b) Gheorghie, R.; Cucos, P.; Andruh, M.; Costes, J. P.; Donnadiu, B.; Shova, S. *Chem.—Eur. J.* **2006**, *12*, 187. (c) Sun, Y. Q.; Zhang, J.; Chen, Y. M.; Yang, G. Y. *Angew. Chem., Int. Ed.* **2005**, *44*, 2. (d) Li, J. R.; Bu, X. H.; Zhang, R. H. *Inorg. Chem.* **2004**, *43*, 237. (e) Shin, D. M.; Lee, I. S.; Lee, Y. A.; Chung, Y. K. *Inorg. Chem.* **2003**, *42*, 2977. (f) Pan, L.; Adams, K. M.; Hernandez, H. E.; Wang, X. T.; Zheng, C.; Hattori, Y.; Kaneko, K. *J. Am. Chem. Soc.* **2003**, *125*, 3062. (g) Uemura, K.; Kitagawa, S.; Kondo, M.; Fukui, K.; Kitaura, R.; Chang, H. C.; Mizutani, T. *Chem.—Eur. J.* **2002**, *8*, 3586. (h) Chu, D. Q.; Xu, J. Q.; Duan, L. M.; Wang, T. G.; Tang, A. Q.; Ye, L. *Eur. J.*

*Inorg. Chem.* **2001**, *1135*. (i) Hagrman, P. J.; Hagrman, D.; Zubieta, J. *Angew. Chem., Int. Ed.* **1999**, *38*, 2638.

(3) (a) Chelebaeva, E.; Larionova, J.; Guari, Y.; Ferreira, R. A. S.; Carlos, L. D.; Paz, F. A. A.; Trifonov, A.; Guerin, C. *Inorg. Chem.* **2009**, *48*, 5983. (b) Harbuzaru, B. V.; Corma, A.; Rey, F.; Atienzar, P.; Jorda, J. L.; Garcia, H.; Ananias, D.; Carlos, L. D.; Rocha, J. *Angew. Chem., Int. Ed.* **2008**, *47*, 1080. (c) Chelebaeva, E.; Larionova, J.; Guari, Y.; Ferreira, R. A. S.; Carlos, L. D.; Paz, F. A. A.; Trifonov, A.; Guerin, C. *Inorg. Chem.* **2008**, *47*, 775. (d) Luo, F.; Batten, S. R.; Che, Y. X.; Zheng, J. M. *Chem.—Eur. J.* **2007**, *13*, 4948. (e) de Lill, D. T.; de Bettencourt-Dias, A.; Cahill, C. L. *Inorg. Chem.* **2007**, *46*, 3960.

(4) (a) Leong, W. L.; Vittal, J. J. *Chem. Rev.* **2011**, *111*, 688. (b) Biradha, K.; Sarkar, M.; Rajput, L. *Chem. Commun.* **2006**, 4169. (c) Sokolov, A. N.; MacGillivray, L. R. *Cryst. Growth Des.* **2006**, *6*, 2615. (d) Chen, C.-L.; Kang, B.-S.; Su, C.-Y. *Aust. J. Chem.* **2006**, *59*, 3. (e) Han, L.; Hong, M. *Inorg. Chem. Commun.* **2005**, *8*, 406. (f) Serrano, J. L.; Sierra, T. *Coord. Chem. Rev.* **2003**, *242*, 73. (g) Khlobystov, A. N.; Blake, A. J.; Champness, N. R.; Lemenovskii, D. A.; Majouga, A. G.; Zyk, N. V.; Schröder, M. *Coord. Chem. Rev.* **2001**, *222*, 155. (h) Chen, C.-T.; Suslick, K. S. *Coord. Chem. Rev.* **1993**, *128*, 293.

(5) (a) Xia, J.; Zhao, B.; Wang, H.-S.; Shi, W.; Ma, Y.; Song, H.-B.; Cheng, P.; Liao, D.-Z.; Yan, S.-P. *Inorg. Chem.* **2007**, *46*, 3450. (b) Yang, X.-P.; Jones, R. A. *J. Am. Chem. Soc.* **2005**, *127*, 7686. (c) Sabbatini, N.; Guardigi, M.; Bolletta, F.; Manet, I.; Ziessel, R. *Angew. Chem., Int. Ed. Engl.* **1994**, *33*, 1501.

(6) (a) Ren, Y.-P.; Long, L.-S.; Mao, B.-W.; Yuan, Y.-Z.; Huang, R.-B.; Zheng, L.-S. *Angew. Chem., Int. Ed.* **2003**, *42*, 532. (b) Deacon, G. B.; Forsyth, C. M.; Behrsing, T.; Konstas, K.; Forsyth, M. *Chem. Commun.* **2002**, 2820. (c) Liu, S.; Meyers, E. A.; Shore, S. G. *Angew. Chem., Int. Ed.* **2002**, *41*, 3609. (d) Ma, B.-Q.; Gao, S.; Su, G.; Xu, G.-X. *Angew. Chem., Int. Ed.* **2001**, *40*, 434. (e) Lisowski, J.; Starynowicz, P. *Inorg. Chem.* **1999**, *38*, 1351. (f) Liu, J.; Meyers, E. A.; Cowan, J. A.; Shore, S. G. *Chem. Commun.* **1998**, 2043. (g) Coronada, E.; Gómez-García, C.-J. *Chem. Rev.* **1998**, *98*, 273. (h) Stumpf, H. O.; Ouahab, L.; Pei, Y.; Bergerat, P.; Kahn, O. *J. Am. Chem. Soc.* **1994**, *116*, 3866.

(7) (a) Ye, J.; Zhang, J.; Ning, G.; Tian, G.; Chen, Y.; Wang, Y. *Cryst. Growth Des.* **2008**, *8*, 3098. (b) Yang, X.-P.; Jones, R. A.; Rivers, J. H.; Lai, R. P. *Dalton Trans.* **2007**, 3936. (c) Ye, J. W.; Wang, J.; Zhang, J. Y.; Zhang, P.; Wang, Y. *CrystEngComm* **2007**, *9*, 515. (d) Weng, D.; Zheng, X.; Li, L.; Yang, W.; Jin, L. *Dalton Trans.* **2007**, 4822. (e) de Lill, D. T.; Cahill, C. L. *Chem. Commun.* **2006**, 494. (f) Chen, X. Y.; Zhao, B.; Shi, W.; Xia, J.; Cheng, P.; Shi, W.; Liao, D. Z.; Yan, S. P.; Jiang, Z. H. *Chem. Mater.* **2005**, *17*, 2866. (g) Zhang, Z.-H.; Okamura, T.; Hasegawa, Y.; Kawaguchi, H.; Kong, L.-Y.; Sun, W.-Y.; Ueyama, N. *Inorg. Chem.* **2005**, *44*, 6219. (h) Wang, Y.; Zhang, L.; Jin, L.; Gao, S.; Lu, S. *Inorg. Chem.* **2003**, *42*, 4985.

(8) (a) de Lill, D. T.; de Bettencourt Dias, A.; Cahill, C. L. *Inorg. Chem.* **2007**, *46*, 3960. (b) Théry, P. *CrystEngComm* **2007**, *9*, 460. (c) Zhu, W.-H.; Wang, Z.-M.; Gao, S. *Dalton Trans.* **2006**, 765. (d) Manna, S. C.; Zangrando, E.; Bencini, A.; Benelli, C.; Chaudhuri, N. R. *Inorg. Chem.* **2006**, *45*, 9114. (e) Daniel, T. L.; Noel, S. G.; Christopher, L. C. *Inorg. Chem.* **2005**, *44*, 258.

(9) (a) Zhu, X.; Lu, J.; Li, X.; Gao, S.; Li, G.; Xiao, F.; Cao, R. *Cryst. Growth Des.* **2008**, *8*, 1897. (b) Kelly, N. R.; Goetz, S.; Batten, S. R.; Kruger, P. E. *CrystEngComm* **2008**, *10*, 68. (c) Huang, Y.-G.; Jiang, F.-L.; Yuan, D.-Q.; Wu, M.-Y.; Gao, Q.; Wei, W.; Hong, M.-C. *Cryst. Growth Des.* **2008**, *8*, 166. (d) Law, G.-L.; Wong, K.-L.; Yang, Y.-Y.; Yi, Q.-Y.; Jia, G.; Wong, W.-T.; Tanner, P. A. *Inorg. Chem.* **2007**, *46*, 9754. (e) Sun, Y.-Q.; Yang, G.-Y. *Dalton Trans.* **2007**, 3771. (f) Pan, L.; Olson, D. H.; Ciemnomolonski, L. R.; Heddy, R.; Li, J. *Angew. Chem., Int. Ed.* **2006**, *45*, 616. (g) Pavel, V.; Peter, C.; Jan, K.; Jakub, R.; Peter, H.; Ivan, L. *Inorg. Chem.* **2005**, *44*, 5591. (h) Sujit, K. G.; Parimal, K. B. *Inorg. Chem.* **2003**, *42*, 8250. (i) Qin, C.; Wang, X. L.; Wang, E. B.; Su, Z. M. *Inorg. Chem.* **2005**, *44*, 7122.

(10) (a) Liu, M. S.; Yu, Q. Y.; Cai, Y. P.; Su, C. Y.; Lin, X. M.; Zhou, X. X.; Cai, J. W. *Cryst. Growth Des.* **2008**, *8*, 4083. (b) Wang, H. S.; Zhao, B.; Zhai, B.; Shi, W.; Cheng, P.; Liao, D. Z.; Yan, S. P. *Cryst. Growth Des.* **2007**, *7*, 1851. (c) Zhao, B.; Gao, H. L.; Chen, X. Y.; Cheng, P.; Shi, W.; Liao, D. Z.; Yan, S. P.; Jiang, Z. H. *Chem.—Eur. J.*

2006, 12, 149. (d) Gao, H. L.; Yi, L.; Zhao, B.; Zhao, X. Q.; Cheng, P.; Liao, D. Z.; Yan, S. P. *Inorg. Chem.* **2006**, 45, 5980. (e) Qin, C.; Wang, X. L.; Wang, E. B.; Su, Z. M. *Inorg. Chem.* **2005**, 44, 7122. (f) Zhao, B.; Yi, L.; Dai, Y.; Chen, X. Y.; Cheng, P.; Shi, W.; Liao, D. Z.; Yan, S. P.; Jiang, Z. H. *Inorg. Chem.* **2005**, 44, 911. (g) Zhao, B.; Cheng, P.; Chen, X. Y.; Cheng, C.; Shi, W.; Liao, D. Z.; Yan, S. P.; Jiang, Z. H. *J. Am. Chem. Soc.* **2004**, 126, 3012. (h) Sujit, K. G.; Parimal, K. B. *Inorg. Chem.* **2003**, 42, 8250.

(11) Pryor, K. E. *Tetrahedron* **1998**, 54, 4107.

(12) Yin, D. X.; Li, Y. F.; Liu, J. G.; Zhang, S. J.; Yang, S. Y. *Chin. Chem. Lett.* **2003**, 14, 1139.

(13) Kelly, N. R.; Goetz, S.; Batten, S. R.; Kruger, P. E. *CrystEngComm* **2008**, 10, 68.

(14) Kelly, N. R.; Goetz, S.; Batten, S. R.; Kruger, P. E. *CrystEngComm* **2008**, 10, 1018.

(15) Lin, X.; Blake, A. J.; Wilson, C.; Sun, X. Z.; Champness, N. R.; George, M. W.; Hubberstey, P.; Mokaya, R.; Schroder, M. J. *Am. Chem. Soc.* **2006**, 128, 10745.

(16) Dawid, U.; Pruchnik, F. P.; Starosta, R. *Dalton Trans.* **2009**, 3348.

(17) SHELXTL, version 5.1; Bruker AXS: Madison, WI, 1998.

(18) Sheldrick, G. M. *SHELXL-97: Program for the Refinement of Crystal Structure*; University of Göttingen: Göttingen, Germany, 1997.

(19) (a) Yang, G. P.; Wang, Y. Y.; Liu, P.; Fu, A. Y.; Zhang, Y. N.; Jin, J. C.; Shi, Q. Z. *Cryst. Growth Des.* **2010**, 10, 1443. (b) Pan, L.; Frydel, T.; Sander, M. B.; Huang, X. Y.; Li, J. *Inorg. Chem.* **2001**, 40, 1271.

(20) Bellamy, L. J. *The Infrared Spectra of Complex Molecules*; Wiley: New York, 1958.

(21) (a) Zhao, B.; Chen, X. Y.; Cheng, P.; Liao, D. Z.; Yan, S. P.; Jiang, Z. H. *J. Am. Chem. Soc.* **2004**, 126, 15394. (b) Gu, X. J.; Xue, D. F. *CrystEngComm* **2007**, 9, 471.

(22) (a) Kirby, A. F.; Foster, D.; Richardson, F. S. *Chem. Phys. Lett.* **1983**, 95, 507. (b) J. C. G. Bünzli. Choppin, G. R. *Lanthanide Probes in life, Chemical and Earth Science. Theory and Practice*; Elsevier Scientific Publishers: Amsterdam, The Netherlands, 1989; Chapter 7 (ref:1.2 IC).

(23) Andruh, M.; Bakalbassis, E.; Kahn, O.; Trombe, J. C.; Porcher, P. *Inorg. Chem.* **1993**, 32, 1616.

(24) (a) Parkar, D. *Coord. Chem. Rev.* **2000**, 205, 109. (b) Kido, J.; Okamoto, Y. *Chem. Rev.* **2002**, 102, 2357. (c) Vicentini, G.; Zinner, L. B.; Zukerman-Schpector, J.; Zinner, K. *Coord. Chem. Rev.* **2000**, 196, 353.